Journal of Magnetic Resonance 193 (2008) 41–48

Contents lists available at ScienceDirect

Journal of Magnetic Resonance

journal homepage: www.elsevier.com/locate/jmr

Cross-term-compensated pulsed-gradient stimulated echo MR with asymmetric gradient pulse lengths

Jürgen Finsterbusch *

Department of Systems Neuroscience, University Medical Center Hamburg-Eppendorf, Hamburg, Germany
Neuroimage Nord, University Medical Centers Hamburg–Kiel–Lübeck, Germany

ARTICLE INFO

Article history:
Received 6 February 2008
Revised 8 April 2008
Available online 11 April 2008

Keywords:
Background gradients
Cross-term compensation
Diffusion
MAGSTE
Generalized MAGSTE

ABSTRACT

The magic asymmetric gradient stimulated echo (MAGSTE) sequence developed to compensate background-gradient cross-terms in the preparation and readout interval independently, assumes identical lengths for the two gradient pulses applied in each interval. However, this approach is rather inefficient if some extra delay time is present in one half of an interval, e.g. as required for special RF excitations or spatial encoding prior to the stimulated echo in MR imaging. Therefore, a generalized version of the sequence is presented that considers different gradient pulse lengths within an interval. It is shown theoretically that (i) for any pulse lengths a "magic" amplitude ratio exists which ensures the desired cross-term compensation in each interval and that (ii) prolonging one of the gradients can deliver a considerably higher diffusion weighting efficiency. These results are confirmed in MR imaging experiments on phantoms and *in vivo* in the human brain at 3 T using an echo-planar trajectory. In the examples shown, typically 10 times higher *b* values can be achieved or an echo time reduction with a 40% signal gain in brain white matter. Thus, in case of asymmetric timing requirements, the generalized MAGSTE sequence with different gradient pulse lengths may help to overcome signal-to-noise limitations in diffusion weighted MR.

1. Introduction

Pulsed-field-gradient NMR [1–3] is widely used in a variety of scientific fields to measure diffusion properties non-invasively [4,5]. However, the measurements are often hampered by macroscopic or microscopic background gradients, in particular in the presence of magnetic field inhomogeneities or in heterogeneous samples [6]. These background gradients interfere with the pulsed gradients used to encode diffusion-related spin displacement, yielding a cross-term as an additional contribution to the diffusion weighting (e.g. [7]).

Because it is difficult to estimate this contribution for microscopic background gradients and to consider it appropriately when determining diffusion coefficients, several pulse sequences have been developed that inherently have a vanishing cross-term [8,9]. The approach of Karlicek and Lowe extends the standard spin-echo diffusion weighting sequence by using multiple refocusing RF pulses [8]. For the pulsed-gradient stimulated echo (PGSTE) sequence that is commonly used for samples with a T_2 short compared to the desired diffusion time, a similar modification has been presented by Cotts et al. that introduced refocusing RF pulses in the middle of the preparation and the readout interval and used two gradients of opposite polarity for the diffusion weighting in each of the intervals [9]. But this technique can only compensate for cross-terms raising from background gradients that are constant during the diffusion time, i.e. from the preparation to the readout interval. In practice, this assumption is often violated in heterogeneous samples, in particular with respect to the long diffusion times accessible with stimulated echo sequences [10].

To overcome this limitation, the sequence of Cotts et al. has been extended to achieve a compensation of the cross-terms in each of the preparation and readout intervals independently [11]. The technique was termed "magic asymmetric gradient stimulated echo" (MAGSTE) because the compensation is realized by using different amplitudes for the gradients applied in each interval with a certain, so-called "magic", ratio [11–14]. More recently, an extension of MAGSTE has been proposed that involves a third gradient lobe within each interval and delivers an improved diffusion weighting efficiency without sacrificing the cross-term compensation [15]. All these techniques consider the time available for the diffusion gradient pulses to be the same for both pulses of an interval.

However, this timing does not consider the specific needs present in some experiments like MR imaging where additional time prior to the stimulated echo is required for spatial encoding. Fur-

* Address: Institut für Systemische Neurowissenschaften, Geb. S10, Universitätsklinikum Hamburg-Eppendorf, 20246 Hamburg, Germany. Fax: +49 40 42803 9955.
E-mail address: j.finsterbusch@uke.uni-hamburg.de.

1090-7807/$ - see front matter © 2008 Elsevier Inc. All rights reserved.
doi:10.1016/j.jmr.2008.04.016

thermore, most MR imaging measurements *in vivo* are based on echo-planar imaging (EPI) [16] that acquires half of the *k*-space lines prior to the central line which is expected to cover the RF refocused echo. Thus, considerable time must be reserved after the last diffusion gradient pulse. To ensure RF refocusing the corresponding time must also appear in the first half of the readout interval and could be used to prolong the diffusion gradient in this section.

Here, the MAGSTE sequence [11] is generalized by considering different gradient pulse lengths to account for asymmetric delay times within the readout (or preparation) interval as, for instance, may occur in MR imaging or when using special RF excitations. It is shown that for arbitrary gradient pulse lengths (i) a "magic" gradient amplitude ratio exists that ensures nulled cross-terms in each interval and (ii) delivers a higher diffusion weighting efficiency compared to the standard MAGSTE sequence if the gradient pulse with the lower amplitude in the standard MAGSTE is prolonged. This approach allows higher q or b values for a given timing or shorter pulse lengths and echo times with accordingly reduced T_2-related signal losses.

2. Theory

The basic pulse sequence of the standard MAGSTE sequence is shown in Fig. 1a. It is an extension of the stimulated echo sequence where refocusing RF pulses are inserted in the middle of the preparation and readout interval [9]. Diffusion weighting is achieved by two gradient pulses of the same length within each interval symmetrically positioned around the refocusing RF pulses. To achieve the suppression of the background-gradient cross-terms, the two gradients must have the same polarity and a, so-called "magic", amplitude ratio of

$$|\eta| = \frac{\delta^2 + 3\delta\delta_1 + 3\delta_1^2}{5\delta^2 + 9\delta\delta_1 + 3\delta_1^2 + 12(\delta+\delta_1)\delta_2 + 6\delta_2^2} \tag{1}$$

with lower amplitudes for the diffusion gradient pulses following the initial RF excitation in the preparation interval and prior to the stimulated echo in the readout interval, respectively [11].

In MR imaging experiments, the time δ_1 between the last diffusion gradient pulse and the stimulated echo may be rather long, in particular if an EPI trajectory is used for data acquisition. In this case, the diffusion weighting scheme of the standard MAGSTE sequence is rather inefficient because a delay time of δ_1 must also be applied between the last $\pi/2$ excitation and the subsequent gradient pulse (Fig. 1a).

To improve the efficiency, the generalized MAGSTE sequence with different pulse lengths and delay times as shown in Fig. 1b can be used. The first diffusion gradient pulse in the readout interval is prolonged to a duration of δ', only leaving a preceding delay time of δ_3 (Fig. 1b). But this prolongation also requires an adaptation of the pulse amplitude(s) in the interval to retain the desired cross-term compensation.

In order to simplify the corresponding theoretical considerations, rectangular diffusion gradients are assumed in the following paragraphs. The derivations can be performed in a strictly analogous way for trapezoidal gradient pulse shapes yielding additional, rather lengthy expressions of the gradient ramp time(s) which do not add substantial aspects. However, all plots presented in the Results section are based on the equations obtained for trapezoidal gradients.

The cross-term of a background gradient of amplitude g_b with the diffusion gradient pulses within the readout (and preparation) interval of the generalized MAGSTE sequence is given by

$$b_{\text{cross}} = \gamma^2 g_b g_1 \left(\frac{5}{6}\delta^3 + (2\delta_2 + \frac{3}{2}\delta_1)\delta^2 + (\delta_2^2 + 2\delta_1\delta_2 + \frac{1}{2}\delta_1^2)\delta\right) - \gamma^2 g_b g_2 \left(\frac{1}{6}\delta^3 + \frac{1}{2}\delta_1\delta^2 + \frac{1}{2}\delta_1^2\delta + \frac{1}{6}\delta_1^3 - \frac{1}{6}\delta_3^3\right) \tag{2}$$

with the gyromagnetic ratio γ. b_{cross} vanishes for arbitrary g_b if the amplitude ratio of the diffusion gradient pulses, η', is

$$\eta' = \frac{g_1}{g_2} = \frac{\delta^3 + 3\delta_1\delta^2 + 3\delta_1^2\delta + \delta_1^3 - \delta_3^3}{\delta(5\ \delta^2 + (9\delta_1 + 12\delta_2)\ \delta + 3\delta_1^2 + 12\delta_1\delta_2 + 6\delta_2^2)}. \tag{3}$$

This means that a "magic" amplitude ratio exists for any lengths of the two diffusion gradient pulses. Because $\delta' > 0$ and $\delta' + \delta_3 = \delta + \delta_1$, δ_3 is less than $\delta + \delta_1$ and, thus, η' is greater than 0 for any positive δ, δ_1, δ_2, and δ_3, i.e. the two gradients must have the same polarity to null the cross-term. For identical pulse lengths ($\delta\prime = \delta$ or $\delta_3 = \delta_1$), η' simplifies to η as expected.

With decreasing δ_3, the gradient amplitude ratio η' increases and matches a value of 1 for

$$\delta_{3,\text{magic}} = \sqrt[3]{\delta_1^3 - (6\delta_2 + 12\delta_1)\delta_2\ \delta - (6\delta_1 + 12\delta_2)\ \delta^2 - 4\delta^3}, \tag{4}$$

which is the only (real) solution of $\eta' = 1$ and is lower than δ_1. In this case, the two diffusion gradients differ in length but have the same amplitude, i.e. the "magic" amplitude ratio found for the stan-

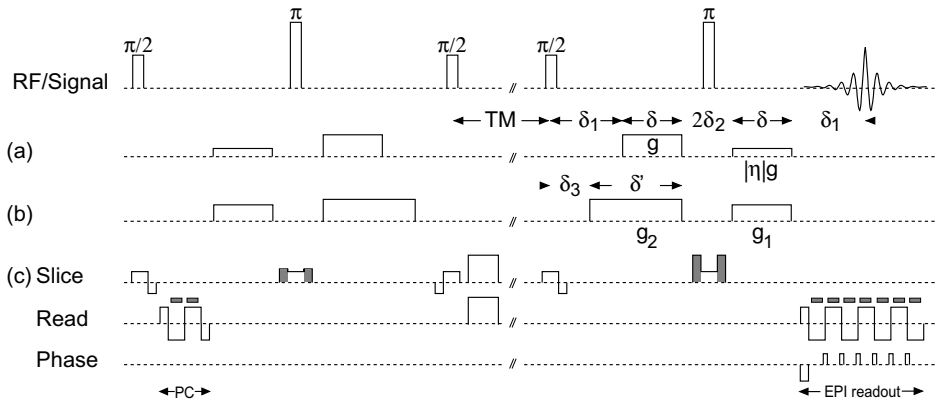

Fig. 1. (a and b) Basic pulse sequences for MAGSTE (a) with identical and (b) different lengths of the diffusion gradient pulses. In the sequence shown in (b), $g_2 = g$ and $g_1 < g_2$ is assumed but depending on the timing parameter this may in general be different (see text). A mirror-symmetric sequence timing is shown for both sequences, however, it should be emphasized that due to the cross-term compensation achieved in each interval independently, preparation and readout intervals with different timings can be combined without sacrificing the cross-term compensation. In (c), the additional gradient pulses applied in the current imaging implementations based on an EPI readout are shown for seven *k*-space lines and two non-phase-encoded reference echoes used for phase-correction (PC). For details see text.

dard MAGSTE sequence is converted to a "magic" pulse length ratio. However, it should be noted that for a δ_1 small compared to δ and/or δ_2 the required delay time δ_3 may be negative, i.e. in contrast to the "magic" amplitude ratio the "magic" length ratio can in general not be realized. For $\delta_3 > \delta_{3,\mathrm{magic}}$, η' is lower than 1 as in standard MAGSTE, i.e. the gradient pulse preceding the stimulated echo has the lower amplitude, while for $\delta_3 < \delta_{3,\mathrm{magic}}$, η' is greater than one and the other gradient has the lower amplitude.

The q value accumulated within the interval with generalized MAGSTE is given by

$$q_{\mathrm{gen}} = g_2\delta' - g_1\delta = g_2(\delta + \delta_1 - \delta_3) - g_1\delta. \tag{5}$$

When considering the ratio of the q values obtained with both sequences

$$\frac{q_{\mathrm{gen}}}{q_{\mathrm{std}}} = \frac{g_2\delta' - g_1\delta}{g\delta(1 - |\,\eta\,|)}, \tag{6}$$

$\delta_3 \geqslant \delta_{3,\mathrm{magic}}$ will be assumed first. g_1 then is chosen as the maximum gradient amplitude g and g_2 according to $g_2 = \eta' g_1 < g_1$. $q_{\mathrm{gen}}/q_{\mathrm{std}}$ in this case is a cubic polynomial in δ_3 that is larger than 1 for any $\delta_3 < \delta_1$, which is the relevant case for MR imaging experiments. This means that using a prolonged gradient delivers higher diffusion weighting than is obtained for identical pulse lengths. Furthermore, the ratio increases with decreasing δ_3, i.e. the largest value is obtained for $\delta_3 = \delta_{3,\mathrm{magic}}$. It should be emphasized that for $\delta_3 > \delta_1$ the efficiency is less than 1 and if the sequence requires a minimum δ_3 that is equal to (or greater than) the minimum δ_1, an artificial prolongation of δ_1 is not beneficial.

In the case $\delta_3 \leqslant \delta_{3,\mathrm{magic}}$, g_2 is chosen as the maximum gradient amplitude g and g_1 according to $g_1 = g_2/\eta' < g_2$. $q_{\mathrm{gen}}/q_{\mathrm{std}}$ as a function of δ_3 then has a single maximum at $\delta_3 = -(\delta + \delta_1)/2$, i.e. a negative value of δ_3. This means that the ratio also increases for decreasing δ_3 in this case and the largest value is obtained for $\delta_3 = 0$ because δ_3 cannot be negative. Thus, it is more efficient to use a longer δ' even if the amplitude of the corresponding pulse has to be reduced because the maximum gradient amplitude is required for the gradient pulse preceding the stimulated echo.

Thus, it can be concluded that (i) the q values obtained with different gradient pulse lengths are larger than that obtained with identical lengths for any $\delta_3 < \delta_1$ and (ii) the best diffusion weighting efficiency is obtained if the shortest possible δ_3 is used which will be referred to as "optimized" pulse lengths in the following sections. It should be noted that these results also hold for the preparation interval if its reversed timing is taken into account appropriately.

The b value accumulated in the preparation or readout interval as shown in Fig. 1b is given by

$$b_{\mathrm{int}} = g_1^2\left(\frac{4}{3}\delta^3 + (2\delta_2 + \delta_1)\delta^2\right) + g_1 g_2(\delta^3 + \delta_1\delta^2 + (\delta_1^2 - \delta_3^2)\delta) + g_2^2\left(\frac{1}{3}\delta^3 + \delta_1\delta^2 + (\delta_1^2 - \delta_3^2)\delta + \frac{2}{3}\delta_3^3 + \frac{1}{3}\delta_1^3 - \delta_1\delta_3^2\right), \tag{7}$$

the b value of the full sequence by

$$b = 2\ b_{\mathrm{int}} + (g_2\delta' - g_1\delta)^2 TM. \tag{8}$$

For simplicity, both equations have been calculated for arbitrary gradient amplitudes g_1 and g_2 and a pulse duration δ', i.e. to obtain the values for optimized pulse lengths, the amplitude ratio η' and $\delta' = \delta + \delta_1 - \delta_3$ need to be considered accordingly.

3. Experimental

The analytical derivations leading to Eqs. (2)–(4) and (7) and the numerical calculations were obtained with Maple 10 (version May 13 2005, Waterloo Maple Inc., Waterloo, Ont., Canada). MR measurements were performed on a 3 T whole-body MR system (Magnetom Trio, Siemens Medical Solutions, Erlangen, Germany) with a maximum gradient amplitude of 40 mT m^{-1} using the body coil for RF transmission and a standard 12-channel head coil for signal reception. MR images of a water phantom and the brain of healthy volunteers were acquired. Informed consent was obtained from all volunteers prior to the examination.

The diffusion weighting schemes shown in Fig. 1a and b were combined with an EPI readout of the stimulated echo as shown in Fig. 1c. All gradient pulses related to in-plane spatial encoding were applied after the end of the last diffusion gradient pulse to avoid cross-terms. The central k-space line of the EPI readout covered the stimulated echo. Three frequency-encoded echoes of the central k-space line were acquired with alternating gradient polarity prior to the diffusion weighting and were used to correct phase distortions related to different gradient pulse polarities. All RF excitations were performed with *sinc*-shaped pulse envelopes and slice-selection gradient pulses. To suppress unwanted signal contributions, (i) the refocusing RF pulses were enclosed by spoiler gradient pulses (gray areas) of different amplitudes in the preparation and readout intervals and (ii) spoiler gradient pulses were applied within the TM interval. Prior to and after the TM interval, dedicated spoiler gradient pulses were omitted and the slice-selection gradient pulses were rephased (as shown in Fig. 1c) for diffusion weighted measurements to avoid cross-terms with the diffusion weighting gradient pulses. Imaging variants of the standard PGSTE sequence and the sequence of Cotts et al. [9]. were obtained analogously.

In addition, two gradient pulses in slice direction with user-selectable amplitudes were inserted covering the full preparation and readout interval, respectively, in order to simulate the effect of background gradients. Amplitudes of up to 400 μT m^{-1} were used in the preparation interval while a maximum of 200 μT m^{-1} was used in the readout interval to avoid excessive image blurring due to signal dephasing along the echo train.

MR images of the water phantom were acquired with a slice thickness of 10 mm, a field-of-view of 180 × 240 mm^2, and a repetition time (TR) of 12,000 ms. Volunteer data were obtained with a slice thickness of 5 mm, a square field-of-view of 192 mm, and a TR of 7500 ms covering 15 sections. No averaging was performed but a preparation scan was applied to achieve steady-state conditions. For all acquisitions an in-plane resolution of 3 × 3 mm^2, a receiver bandwidth of 2160 Hz per pixel, a mixing time (TM) of 300 ms, and echo times (TE) between 64 and 149 ms were used. The echo spacing was 670 μs yielding a total echo train length of 45.6 and 48.6 ms and a δ_1 of 21.1 and 22.6 ms for the water phantom and *in vivo* measurements, respectively.

Diffusion weighting was performed in slice direction and in three orthogonal directions coinciding with the logical imaging coordinate system (phase, read, slice) in the phantom and *in vivo* experiments, respectively, using a maximum amplitude of 35 mT m^{-1} per axis. For the water phantom b values of 500, 1000, and 1500 were used, for MAGSTE with identical pulse lengths with a δ of 11.0 ms and an η of 0.362, for the extension with optimized pulse lengths with a δ of 2.0 ms, a δ' of 20.8 ms (δ_3 2.3 ms), and an η' of 2.05. *In vivo* measurements involved b values of 500 and 1000 s mm^{-2} with a δ of 10.0 ms and an η of 0.384 for identical pulse lengths and a δ of 1.8 ms, a δ' of 22.0 ms (δ_3 2.3 ms), and an η' of 2.48 otherwise. For MAGSTE acquisitions with optimized pulse lengths the shortest δ sufficient to achieve the given b value was used and TE was reduced accordingly by 36 and 33 ms for the water phantom and *in vivo*, respectively, compared to standard MAGSTE.

The apparent diffusion coefficient (ADC) was calculated during the image reconstruction on a voxel-by-voxel basis using software provided by the manufacturer. Thereby, voxels with an intensity below a pre-defined threshold were discarded. For evaluation, the

signal intensity and ADC value averaged over a circular region-of-interest covering more than 1000 pixel in the center of the phantom was used. The standard deviation of the ADC values within the region-of-interest typically was about 0.05×10^{-3} mm^2 s^{-1}. However, the reproducability of the mean ADC value was much better with a variation of less than 0.003×10^{-3} mm^2 s^{-1} observed in eight consecutive measurements with identical parameters. Noise was estimated from the standard deviation of pixel intensities in a region-of-interest covering image background without visible contributions from MR signals.

4. Results

Fig. 2a and b show an example for the gradient pulse amplitudes and lengths (Fig. 2a) and their b value (Fig. 2b) using identical and optimized pulse lengths. For clearness, the time course within the preparation interval is shown, i.e. compared to the readout interval the time course is reversed. Using identical pulse lengths, an amplitude ratio of about 0.33 is required according to Eq. (1). Allowing different pulse lengths, a much longer second gradient (more than double length) can be used with the full amplitude because $\delta_{3,\mathrm{magic}}$ is negative for the selected parameters (Fig. 2a). The amplitude ratio η' then is slightly larger (about 0.43) yielding a minor increment of the amplitude of the first gradient. It is obvious that the q value accumulated in the interval is much larger when using different pulse lengths with the major gain accumulated in the last part of the interval due to the prolonged second gradient.

This also holds for the b value with an almost threefold value at the end of the interval (Fig. 2b), i.e. for a given b value the gradient pulse amplitudes of the generalized sequence shown in Fig. 2a could be reduced by a factor of about $\sqrt{3}$. The b value present at the end of the interval is large compared to the value at the inflexion points (at about 25 ms) which represents the contribution of inner-interval de- and rephasing. This demonstrates that for both schemes most of the b value is related to dephasing in the preparation and rephasing in the readout interval. However, the extension can also be considered to be slightly superior in this context as the relative inner-interval contribution to b is lower.

As shown in Fig. 2c, the cross-term with a background-gradient considered constant during the interval vanishes at the end of the interval in both cases. There are higher absolute intermediate values for the different pulse lengths in the center of the interval but taking again the much higher diffusion weighting into account relative b_{cross} values are smaller.

In Fig. 3a, $\delta_{3,\mathrm{magic}}$, the δ_3 value for which both gradient pulses have the same amplitude, is plotted as a function of δ and δ_1. The values are negative for $\delta_1 \gg \delta$, have a zero crossing for δ_1 being in the order of δ, and are positive for $\delta_1 \ll \delta$, approaching δ_1 for long δ_1 and short δ. For larger δ_2, $\delta_{3,\mathrm{magic}}$ has lower values and the zero crossing is shifted towards larger δ_1 and lower δ, respectively. Plots of the amplitudes of the gradient pulses that ensure the highest diffusion efficiency are presented in Fig. 3b and c for $\delta_3 = \delta_2$ which is expected to be a reasonable assumption for standard experiments. Whereas in the regime of negative $\delta_{3,\mathrm{magic}}$, g_2 has the maximum value and g_1 may be as low as 15% of g_2, the ratio is inverted for large positive $\delta_{3,\mathrm{magic}}$ with g_2 being only several percent of g_1 for long δ_1 and short δ. Where $\delta_{3,\mathrm{magic}} = \delta_2$, the highest efficiency is obtained with both gradients matching the maximum amplitude. This range is shifted with increasing δ_2 similar to $\delta_{3,\mathrm{magic}}$ in Fig. 2a.

Examples of the ratio between the q value accumulated in one of the intervals and the b value of the full sequences are presented in Fig. 4 for $\delta_3 = \delta_2$. For the full parameter range shown, optimized pulse lengths deliver higher q and b values with a ratio ranging from close to 1 for small δ_1 to well above 5 and 10, respectively,

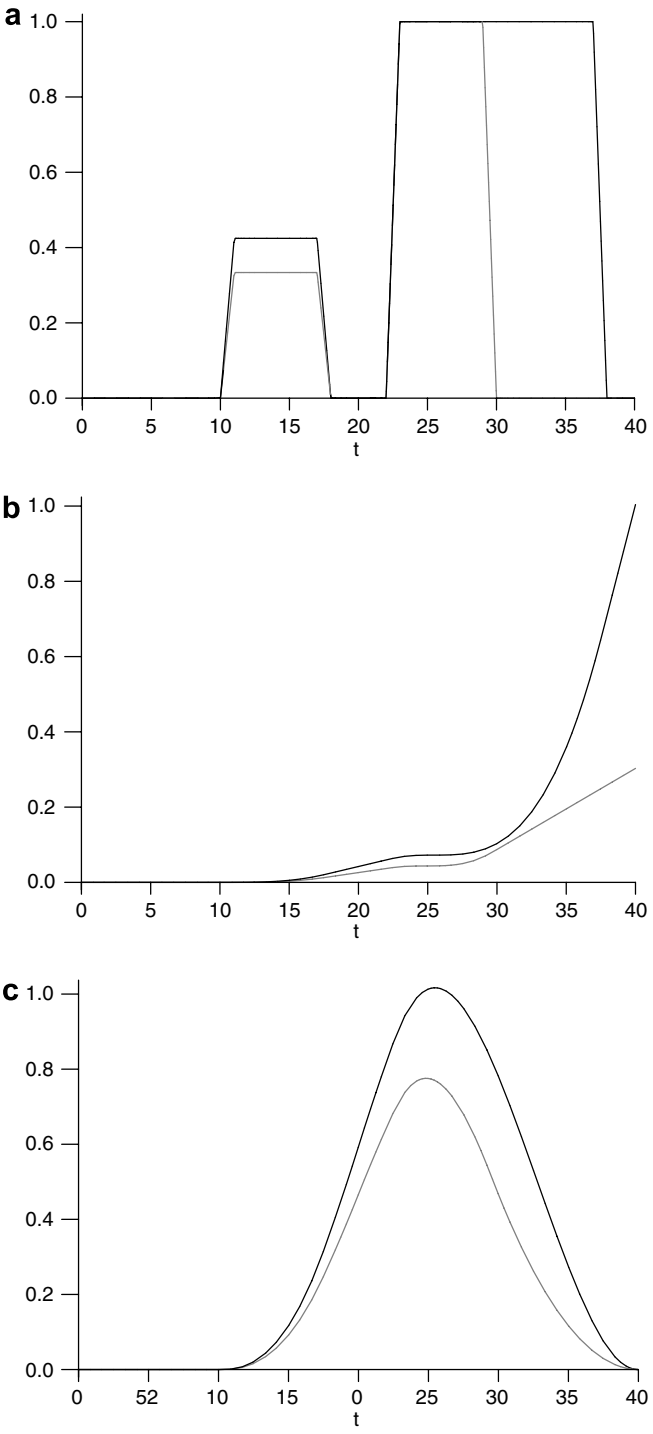

Fig. 2. Schematic time courses (in ms) in the preparation interval for identical (gray) and optimized pulse lengths (black) of (a) the diffusion weighting gradients, (b) their b value, and (c) their cross-term with a constant background-gradient. In this example, a δ of 7 ms, a δ_1 of 10 ms, a gradient ramp time of 1 ms, and a δ_3 of 2 ms was used yielding a δ' of 15 ms. The ordinates are in arbitrary units.

for large δ_1 and small δ with maximum values of about 17 and 200 for the shorter δ_2, respectively (data truncated). This behavior is directly related to the relative prolongation of the diffusion gradient. Where the gradient amplitude ratio is 1, the surface of the q ratio plot has a visible kink that is also observed in the relative amplitudes of Fig. 3a and b. In both plots, the ratios are increased for shorter $\delta_2 = \delta_3$. The b value ratio depends on TM and increases for longer TM, i.e. the b value of the presented extension raises

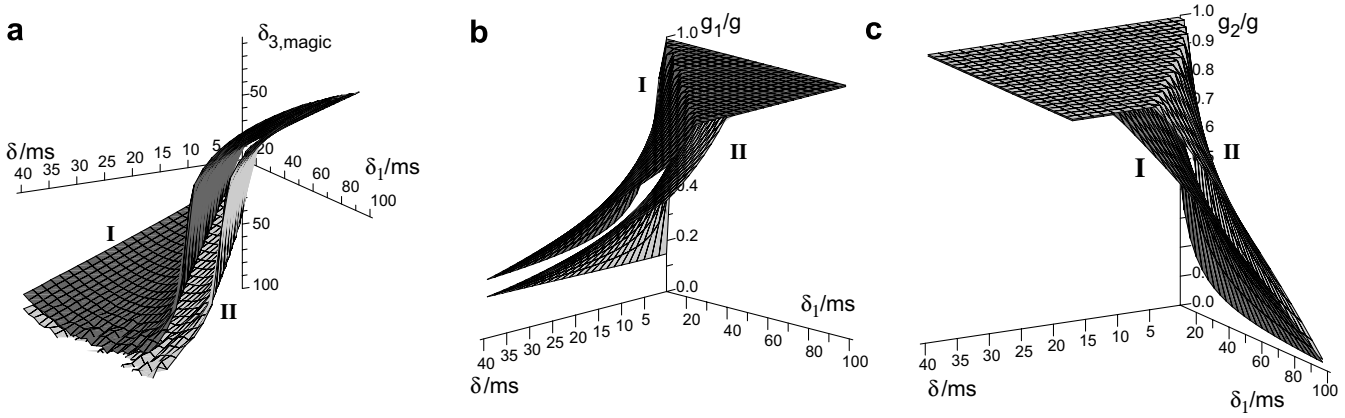

Fig. 3. (a) The δ_3 value for which the "magic" gradient amplitude ratio is 1 vs. δ and δ_1. (b and c) The relative gradient amplitudes of the two diffusion gradients in an interval for optimized gradient pulse lengths with $\delta_2 = \delta_3$. Plots for two different δ_2 of 4 ms (dark gray, I) and 12 ms (light gray, II) are shown, a gradient ramp time of 1 ms was assumed for all plots.

more with TM than for standard MAGSTE. For instance, the ratio grows by about 20% when prolonging TM from 200 to 1000 ms (data not shown).

The higher diffusion weighting efficiency of generalized MAGSTE can also be used to shorten the gradient pulse length δ, and accordingly TE, for a given q or b value. This is in particular important because stimulated echo sequences are preferred for samples with short T_2. Ratios of δ and TE for a given q are shown in Fig. 5. Relative reductions of δ of up to 90% are found for very short δ and long δ_1 (Fig. 5a) but in absolute values may reflect only one millisecond. More crucial is the TE shortening achievable (Fig. 5b) that more directly reflects the signal gain which can be obtained due to reduced T_2 relaxation. Compared to the δ ratio, it looks less impressive but with typical values around 75% and a minimum value of about 50% it is still promising. An even more pronounced improvement can be expected for a given b value because of the higher ratios observed in Fig. 4c. For shorter $\delta_3 = \delta_2$, both ratios shown are reduced, i.e. the efficiency is improved.

Experimental results acquired with diffusion-weighted EPI on a water phantom are presented in Fig. 6. Typical signal-to-noise ratios for the underlying diffusion weighted images were about 24 for the largest b value (1500 s mm^{-2}) and the longest echo time used (149 ms). Without simulated background gradients, all sequences reveal similar ADC values, with mean values of 1.913, 1.935, 1.925, and 1.920 $\times$ 10^{-3} mm^2 s^{-1} in the region-of-interest (Fig. 6a–d). These values are a little bit lower than the value expected from the literature (2.03 $\times$ 10^{-3} mm^2 s^{-1}) [17] for the temperature within the MR room (about 20 °C). A reference measurement without the EPI readout that acquired only one echo per shot with otherwise identical parameters delivered a slightly higher ADC value of 1.951 $\times$ 10^{-3} mm^2 s^{-1} indicating that some of the deviation can be attributed to the gradient pulses of the EPI readout. Doubling the spoiler gradient moments did not change the ADC values which makes it unlikely that the spoiler and the (weaker) slice-selection gradient pulses have a significant influence on the calculated ADC values. Most likely, an imperfect gradient scaling may explain the observed underestimation which corresponds to gradient pulse amplitudes 2% lower than the nominal value.

Switching pulsed gradients to simulate background gradients with the same or different amplitudes in the preparation and readout interval reveals the differences between the sequences. For the standard PGSTE measurement the observed ADC value is reduced to 1.847 $\times$ 10^{-3} mm^2 s^{-1} for identical background gradient amplitudes (Fig. 6e) while the other sequences only exhibit a minor change of 0.003 $\times$ 10^{-3} mm^2 s^{-1} or below (Fig. 6f–h) demonstrating their cross-term compensation capability. Using different amplitudes of the simulated background gradients in the prepara-

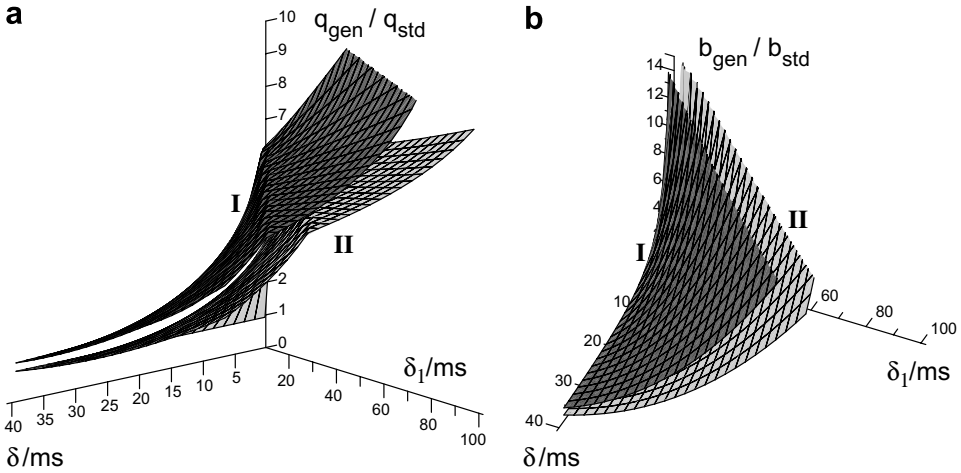

Fig. 4. Relative (a) q and (b) b values for optimized compared to identical pulse lengths for two different $\delta_2 = \delta_3$ of 4 ms (dark gray, I) and 12 ms (light gray, II) and with a gradient ramp time of 1 ms. Plots were truncated for ratios of 10 and 15, respectively. The b values were calculated for a TM of 200 ms.

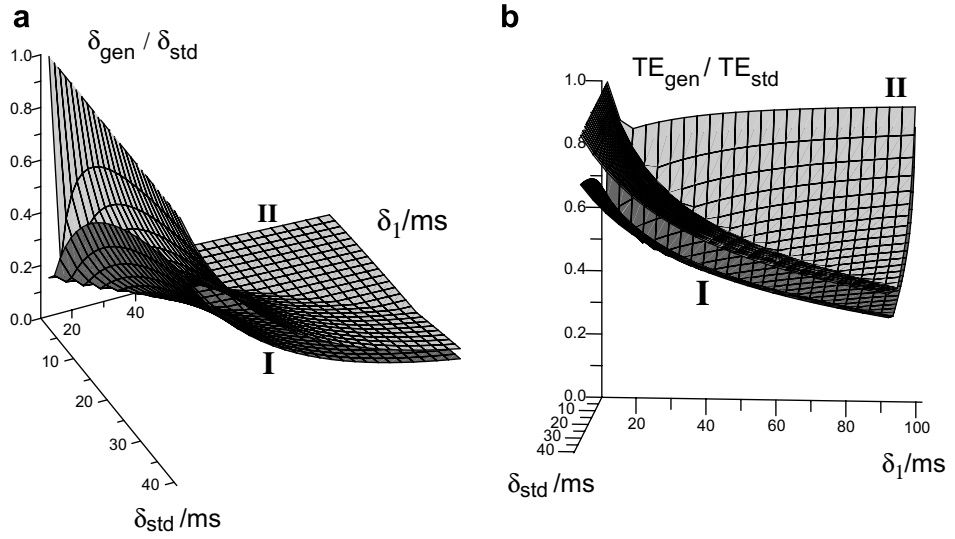

Fig. 5. Relative (a) δ and (b) TE values for a given q value required for optimized compared to identical pulse lengths for two different $\delta_2 = \delta_3$ of 4 ms (dark gray, I) and 12 ms (light gray, II) and a gradient ramp time of 1 ms.

tion and readout intervals yielded an almost complete signal dephasing for the PGSTE sequence as is demonstrated by the diffusion weighted image shown in Fig. 6i. The pronounced dephasing present even for very low amplitude differences of the simulated background gradients did not allow to calculate ADC maps for the PGSTE sequence. For the sequence of Cotts et al. (Fig. 6j) the ADC is estimated to 1.891×10^{-3} mm^2 s^{-1} in this setting, reflecting the limitation of its cross-term compensation to identical background gradients in both intervals. In contrast, the MAGSTE sequences exhibit only a minor change to 1.931 and 1.924×10^{-3} mm^2 s^{-1}, respectively, which demonstrates the desired cross-term compensation of both settings.

In Fig. 6, the higher diffusion weighting efficiency obtained for MAGSTE with optimized pulse lengths was used to shorten δ and reduce the echo time from 147 to 118 ms. If the gradient pulse length δ had been used with the same amplitude as for identical pulse lengths, about 14 times higher b values would have been achieved, i.e. about 7450–23,100 s mm^{-2} instead of 500–1500 s mm^{-2}.

Fig. 7 shows diffusion weighted MR images of the brain of a healthy volunteer obtained *in vivo*. The improved signal-to-noise ratio achieved with optimized (Fig. 7c and d) compared to identical pulse lengths (Fig. 7a and b) is obvious and can be estimated to about 40% in frontal white matter (10.9 vs. 7.7). While for identical

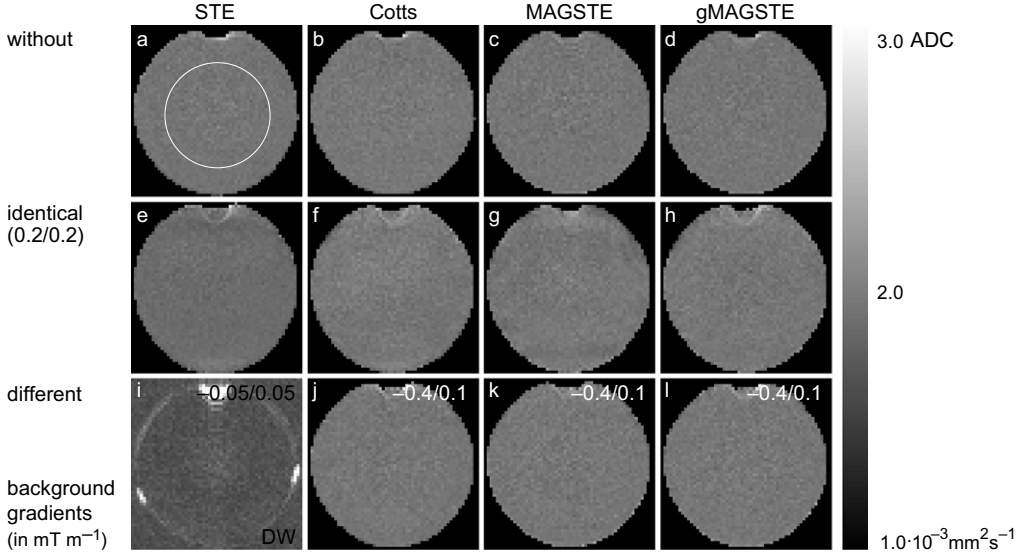

Fig. 6. (a–h and j–l) Maps of the apparent diffusion coefficient obtained in a water phantom with (from left to right) standard PGSTE, the sequence of Cotts et al., standard and generalized MAGSTE (gMAGSTE) with an EPI trajectory. In (e–h) and (j–l) pulsed gradients were switched to simulate background gradients with identical (+0.2 mT m^{-1}) and different amplitudes (−0.4 and +0.1 mT m^{-1}) in the preparation and readout intervals, respectively. (i) represents a diffusion weighted (DW) image ($b = 500$ s mm^{-2}) acquired with the PGSTE sequence and simulated background-gradient amplitudes of −0.05 and +0.05 mT m^{-1} in the preparation and readout intervals which shows the severe signal dephasing present even for low amplitude differences that did not allow to calculate ADC maps. All measurements were performed with the shortest δ and echo times possible for the desired diffusion weighting in order to minimize cross-term effects, yielding 7.6, 3.6, 11.0, and 2.0 ms for δ and 64, 118, 147, 111 ms for the echo time for the PGSTE sequence, the sequence of Cotts et al., the standard and the generalized MAGSTE sequence, respectively. The circle represents the region-of-interest used for the ADC comparisons.

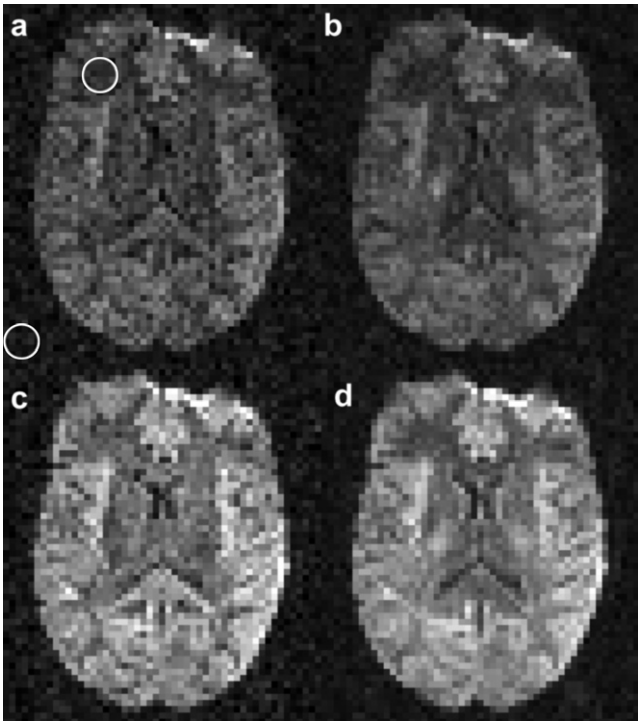

Fig. 7. Diffusion weighted images of the brain of a healthy volunteer obtained with MAGSTE involving (a and b) identical and (c and d) optimized pulse lengths and an EPI trajectory for a b value of 1000 s mm^{-2}. (a and c) Represent single-shot images (without averaging) acquired with diffusion weighting in slice direction (490 ms per section), (b and d) the geometric mean of three single-shot images acquired with diffusion weighting in three orthogonal directions, i.e. so-called trace-weighted images (22.5 s for 15 sections). The gray scaling of all images is identical, i.e. the brighter appearance of (c) and (d) reflects the improved signal-to-noise ratio (SNR). The circles represent the regions-of-interest used for the SNR estimation.

pulse lengths gradient pulses with a duration of 10.0 ms are required in each interval for the given b value, δ can be reduced to 1.8 ms when using optimized pulse lengths and a δ' of 22.0 ms. With this shortening, TE can be reduced by 33 ms (from 149 to 116 ms) yielding the mentioned signal gain. If averaging is required to accumulate sufficient signal the observed gain corresponds to halvening the total measurement time.

5. Discussion

It has been shown that a "magic" gradient amplitude ratio that compensates for background-gradient cross-terms in PGSTE in the preparation and readout interval independently can be found for any given gradient pulse lengths. This can be considered as a generalization of the MAGSTE method that covered the special case of identical pulse lengths. The advantage of the generalized sequence is that it can deliver a higher diffusion weighting efficiency, i.e. it allows higher q or b values for a given timing or a shorter echo time for given q or b. This is of particular importance because PGSTE sequences are usually applied to samples with short T_2.

The improvement requires that the delay time between the first or last gradient pulse and the initial RF excitation (in the preparation interval) or the stimulated echo (in the readout interval), respectively, is longer than its counterpart in the corresponding interval ($\delta_3 < \delta_1$). This situation is typically present in the readout interval of MR imaging experiments due to the pre-dephasing gradient pulses and k-space lines acquired prior to the stimulated echo and has been demonstrated for the EPI trajectory that is commonly used for diffusion weighted imaging. The benefit of the approach with different pulse lengths depends on the asymmetry of these delay times and is therefore less pronounced for other single-shot techniques, like fast spin-echo imaging [18,19], or imaging sequences covering only one k-space line per shot. However, such an asymmetry may also be present in the preparation interval when using long RF excitations like adiabatic [20,21] or multi-dimensional RF excitations [22–24].

Although a mirror-symmetric timing of the preparation and readout interval has been used in the current study, different timings can be used in the two intervals. If the required delay times are symmetric within one of the intervals, the standard MAGSTE approach should be used while different pulse lengths should be applied only in intervals with asymmetric delay times $\delta_3 < \delta_1$ and with the shortest possible δ_3. A potential drawback of combining dedicated timings could be the different sensitivity to background gradients that vary on the time scale of an interval.

The "magic" amplitude ratio may yield 1, i.e. the gradient pulses differ only by their pulse length. Analogous to the "magic" amplitude ratio, this case can be considered as a "magic" pulse length ratio. However, it is not realizable for every timing chosen.

The amplitude of the simulated background gradients used to demonstrate the cross-term compensation capability of the MAGSTE schemes could be considered low compared to the background gradients that may be present in inhomogenous samples, in particular if they are non-biological. In the imaging experiments performed, the amplitude is limited by the dephasing effect of the simulated background gradients which causes a signal loss for the outer k-space lines which converts to a considerable image blurring for values of 1 mT m^{-1} and beyond. First, this effect is independent of the diffusion preparation (MAGSTE, PGSTE, or other) and represents a limitation of the EPI readout which depends on the trajectory duration and can be ameliorated by using shorter echo trains or a different imaging trajectory. More important, the simulated background gradient is a pulsed, macroscopic gradient. Its dephasing is effective on the macroscopic dimension of the sample which yields a much more pronounced effect than a corresponding microscopic gradient. For instance, a simulated (macroscopic) gradient of 1 mT m^{-1} which is applied to a 100 mm phantom, induces a distribution of the magnetic flux density B of 0.1 mT within the sample. If microscopic field inhomogeneities present on the scale of 0.1 mm are expected to cause a similar B distribution a gradient of 100 mT m^{-1} is required. Thus, the constraints to imaging experiments are less restrictive for microscopic gradients and are not expected to limit applications to biological tissue.

It should be kept in mind that MAGSTE sequences can only fully compensate for cross-terms of background gradients that are constant during each of the intervals. But the higher efficiency obtained when using different pulse lengths may also be considered superior to the symmetric case because for a given diffusion weighting (i) lower intermediate cross-terms appear during the intervals and (ii) the echo time can be reduced. Thus, it is expected that the asymmetric sequence is less sensitive to background gradients changing within an interval. Similarly, cross-terms of the diffusion gradient with the slice-selection and spoiler gradient pulses of the refocusing RF in the center of each interval are also expected to be reduced. Because the major part of the dephasing in the preparation interval and rephasing in the readout interval is performed after and prior to the refocusing RF, respectively, q values of the diffusion gradient pulses, and accordingly their cross-terms with the other gradient pulses, are lower during this period. Cross-terms of the background gradients with the gradients of the echo-planar readout are not reduced or compensated but are also not expected to have influence on the ADC calculation as they are independent of the diffusion weighting gradients.

The combination of the presented sequence with the recently proposed extension of the MAGSTE sequence with symmetric de-

lay times [15] that delivers an improved diffusion weighting by introducing a third gradient lobe could be promising. Here, the gradient pulse with the lower amplitude, depending on the exact timing parameters either the first or the second in the interval, could be shortened, and an additional gradient lobe of opposite polarity inserted to further increase the diffusion weighting. However, the analytical calculation of the gradient pulse lengths and amplitudes required to ensure the cross-term compensation seems to be very tedious and the improvement achieved is expected to be considerably lower than that found in the current work.

6. Conclusions

A generalized "magic" amplitude ratio has been found for PGSTE experiments with arbitrary gradient pulse lengths that ensures compensation of background-gradient cross-terms in the preparation and readout interval independently. In case of asymmetric delay times in an interval, using different gradient pulse lengths delivers a higher diffusion weighting efficiency. It therefore may help to overcome current limitations in PGSTE, in particular for MR imaging using an echo-planar trajectory.

Acknowledgments

Parts of this work were supported by Deutsche Forschungsgemeinschaft and Bundesministerium für Bildung und Forschung (Neuroimage Nord).

References

[1] E.O. Stejskal, J.E. Tanner, Spin diffusion measurements: spin echoes in the presence of a time-dependent field gradient, J. Chem. Phys. 42 (1965) 288–292.
[2] W.S. Price, Pulsed field gradient nuclear magnetic resonance as a tool for studying translational diffusion: Part I. Basic theory, Concepts Magn. Reson. 9 (1997) 299–336.
[3] W.S. Price, Pulsed field gradient nuclear magnetic resonance as a tool for studying translational diffusion: Part II. Experimental aspects, Concepts Magn. Reson. A 10 (1998) 197–237.
[4] J. Kärger, P. Heitjans (Eds.), Diffusion in Condensed Matter—Methods, Materials, Models, Springer-Verlag, Berlin–Heidelberg, 2005.
[5] T. Moritani, S. Ekholm, P.-L. Westesson, Diffusion-Weighted MR Imaging of the Brain, Springer-Verlag, Berlin–Heidelberg, 2005.
[6] J. Zhong, R.P. Kennan, J.C. Gore, Effects of susceptibility variations on NMR measurements of diffusion, J. Magn. Reson. 95 (1991) 133–139.
[7] G. Zheng, W.S. Price, Suppression of background gradients in (B0 gradient-based) NMR diffusion experiments, Concepts Magn. Reson. A 30 (2007) 261–277.
[8] R.F. Karlicek Jr., I.J. Lowe, A modified pulsed gradient technique for measuring diffusion in the presence of large background gradients, J. Magn. Reson. 37 (1980) 75–91.
[9] R.M. Cotts, M.J.R. Hoch, T. Sun, J.T. Markert, Pulsed field gradient stimulated echo methods for improved NMR diffusion measurements in heterogeneous systems, J. Magn. Reson. 83 (1989) 252–266.
[10] J.G. Seland, G.H. Sørland, K. Zick, B. Hafskjold, Diffusion measurements at long observation times in the presence of spatially variable internal magnetic field gradients, J. Magn. Reson. 146 (2000) 14–19.
[11] P.Z. Sun, J.G. Seland, D. Cory, Background gradient suppression in pulsed gradient stimulated echo measurements, J. Magn. Reson. 161 (2003) 168–173.
[12] P.Z. Sun, A.S. Seth, J. Zhou, Analysis of the magic asymmetric gradient stimulated echo sequence with shaped gradients, J. Magn. Reson. 171 (2004) 324–329.
[13] P. Galvosas, F. Stallmach, J. Kärger, Background gradient suppression in stimulated echo NMR diffusion studies using magic pulsed field gradient ratios, J. Magn. Reson. 166 (2004) 164–173.
[14] P.Z. Sun, Improved diffusion measurement in heterogeneous systems using the magic asymmetric gradient stimulated echo (MAGSTE) technique, J. Magn. Reson. 187 (2007) 177–183.
[15] J. Finsterbusch, Improved diffusion-weighting efficiency of pulsed gradient stimulated echo MR measurements with background gradient cross-term suppression, J. Magn. Reson. 191 (2008) 282–290.
[16] P. Mansfield, Multi-planar image formation using NMR spin echoes, J. Phys. C 10 (1977) 349–352.
[17] H. Weingärtner, Self diffusion in liquid water. A reassessment, Z. Phys. Chem. 132 (1982) 129–149.
[18] J. Hennig, A. Nauerth, H. Friedburg, RARE imaging: a fast method for clinical MR, Magn. Reson. Med. 3 (1986) 823–833.
[19] D.G. Norris, P. Börnert, T. Reese, D. Leibfritz, On the application of ultra-fast RARE experiments, Magn. Reson. Med. 27 (1992) 142–164.
[20] M.S. Silver, R.I. Josephs, D.I. Hoult, Highly selective $\pi/2$ and π pulse generation, J. Magn. Reson. 59 (1984) 347–351.
[21] R.A. de Graaf, K. Nicolay, M. Garwood, Single-shot B1-insensitive slice selection with a gradient-modulated adiabatic pulse, Magn. Reson. Med. 35 (1996) 652–657.
[22] P.A. Bottomley, C.J. Hardy, Two-dimensional spatially selective spin inversion and spin-echo refocusing with a single nuclear magnetic resonance pulse, J. Appl. Phys. 62 (1987) 4284–4290.
[23] J. Pauly, D. Nishimura, A. Macovski, A *k*-space analysis of small-tip-angle excitations, J. Magn. Reson. 81 (1989) 43–56.
[24] C.J. Hardy, H.E. Cline, Spatial localization in two dimensions using NMR designer pulses, J. Magn. Reson. 82 (1989) 647–654.